A Neurofuzzy Algorithm-Based Advanced Bilateral Controller for Telerobot Systems

Dong-hyuk Cha and Hyung Suck Cho

Abstract: The advanced bilateral control algorithm, which can enlarge a reflected force by combining force reflection and compliance control, greatly enhances workability in teleoperation. In this scheme the maximum boundaries of a compliance controller and a force reflection gain guaranteeing stability and good task performance greatly depend upon characteristics of a slave arm, a master arm, and an environment. These characteristics, however, are generally unknown in teleoperation. It is, therefore, very difficult to determine such maximum boundary of the gain. The paper presented a novel method for design of an advanced bilateral controller. The factors affecting task performance and stability in the advanced bilateral controller were analyzed and a design guideline was presented. The neurofuzzy compliance model (NFCM)-based bilateral control proposed herein is an algorithm designed to automatically determine the suitable compliance for a given task or environment. The NFCM, composed of a fuzzy logic controller (FLC) and a rule-learning mechanism, is used as a compliance controller. The FLC generates compliant motions according to contact forces. The rule-learning mechanism, which is based upon the reinforcement learning algorithm, trains the rule-base of the FLC until the given task is done successfully. Since the scheme allows the use of large force reflection gain, it can assure good task performance. Moreover, the scheme does not require any priori knowledge on a slave arm dynamics, a slave arm controller and an environment, and thus, it can be easily applied to the control of any telerobot systems. Through a series of experiments effectiveness of the proposed algorithm has been verified.

Keywords: neurofuzzy, telerobot, bilateral, force reflection, compliance

I. Introduction

A telerobot system is generally composed of a master arm controlled by a human operator and a slave arm which duplicates the motion of the master arm and performs actual works in a remote site. In a typical telerobot system with no force reflection or compliance control, a stiff slave arm strictly follows the motion of a master arm. To achieve more complex tasks, however, such a system may be unsuitable because of insufficient information on the working environment. The forces exerted by a slave arm interacting with the environment contain a lot of information on the teleoperation processes or working environments. The use of force information, therefore, can greatly improve the task performance. Two major techniques that utilize the contact forces are compliance control and bilateral control [1].

In compliance control systems [2]-[5], the contact forces are not reflected to an operator but used for compliance control of a slave arm. An operator assigns reference trajectory to a slave arm through a master arm and the forces are fed back to a compliance controller. The compliance controller, then, generates corrective motions and these are superimposed to the reference trajectory, and as a result, a modified reference trajectory is generated. In bilateral control systems [6]-[7], the contact forces are reflected to a human operator via a master arm so that he/she can correct his/her motions according to these forces. Such a system is also called as a force reflection system and the force reflection can significantly enhance the task performance. The larger the force reflection gain is, the bigger the reflected force becomes, however, the gain should be bounded into a certain value because of the stability problem [8].

To enlarge the reflected force, many advanced bilateral control algorithms have been proposed by combining the bilateral control and the compliance control [8]-[11]. In these schemes, a slave arm becomes more compliant by adopting compliance control technique, and therefore, it is possible to enlarge the reflected force. Thus, good task performance can be assured. In spite of the previous studies, there still remains unsolved problems such as: how to find out the suitable compliance of a slave arm and how to implement it under the uncertain characteristics of a slave arm and working environments, which are inevitable in most of teleoperation tasks. In an advanced bilateral control system, the compliance greatly affects the task performance. The larger the compliance is the bigger reflected force can assure. But too large compliance can cause stability problem. The maximum boundary of the compliance guaranteeing stability greatly depends upon the force reflection gain, characteristics of the environment and the slave arm. In normal practice, therefore, it is very difficult to determine such maximum boundary of the compliance.

To overcome these difficulties the proposed algorithm automatically determines the compliance in an advanced bilateral controller. The neurofuzzy compliance model(NFCM)-based bilateral controller proposed herein can finds out a suitable compliance for a given task or environment. The NFCM, composed of a fuzzy logic controller (FLC) and a rule-learning mechanism, is used as a compliance controller in this scheme. The FLC generates compliant motions according to contact forces while the rule-learning mechanism, which is based upon the reinforcement learning algorithm [12]-[13], trains the rule-base of the FLC until the given task is done successfully. Since the scheme allows the use of large force reflection gain, it can assure good task performance. Moreover the scheme dose not require any priori knowledge on a slave

Manuscript received: May 20, 2001, Accepted: Aug. 27, 2001.

Dong-hyuk Cha: Dept. of Control and Measurement Engineering, Korea Polytechnic University (dhcha@kpu.ac.kr)

Hyung Suck Cho: Dept. of Mechanical Engineering, KAIST (hscho@lca.kaist.ac.kr)

※This work was supported by Korea Research Foundation Grant (KRF-99-003-E0062).

arm dynamics, a slave arm controller and an environment, and thus, it can be easily applied to the control of any telerobot systems contacting with an environment having unknown stiffness. The effectiveness of the proposed algorithm has been verified thorough a series of experiments.

The paper is organized as follows: a telerobot system used in the study is described in section 2. In section 3, the factors affecting task performance and stability are briefly discussed to find a design guideline of an advanced bilateral controller. The structure of the NFCM-based bilateral controller is described in section 4. The experimental results and discussions are presented in section 5. Finally, some conclusions are made in section 6.

II. Description of a telerobot system

Fig. 1 shows a telerobot system developed at the Laboratory for Control Systems and Automation in the Korea Advanced Institute of Science and Technology. The system consists of a force reflective master arm, a slave arm and a system controller. The master arm has a vertical articulated structure with three degrees of freedom (d.o.f). Three D.C. servo motors with harmonic drives are mounted in each axis. To reduce friction, each motor is directly connected to the rotational shaft of each axis. To enhance maneuverability, balancing weights are attached to the second and third axes. Three axis-control boards are developed as torque controllers. The slave arm is a six-d.o.f industrial robot (Samsung, FARA A1-U) with vertical articulated structure.

A six-axes force/torque sensor (ATI, FT 30/100) is attached at the end of the slave arm to measure the force/moment. To provide visual information of the contact force, a force level indicator composed of 16 light emitting diodes (LED) with a bar graph arrangement is installed at the operator site. Although the human operator can feel the contact force through the master arm, addition of visual feedback of force can significantly enhance task performance during the experiments. To monitor the slave environment, a CCTV camera is installed at the ceiling of the working site.

The telerobot system controller implemented by a PC486/DX2-66 is composed of a master arm kinematics routine, a workspace mapping routine, a slave arm inverse kinematics routine, a compliance controller and a force reflection controller. Since the master and slave arms have kinematically different structures, workspace mapping is required so that a position of the master arm, X_M, can be appropriately transformed to the corresponding space of the slave arm, X_R. The detailed algorithm is similar to that described in [14]. The detailed structures of the compliance controller and the force reflection controller are described in the following section. The master and slave controllers are connected with a main PC through the PC-AT bus via two parallel I/O boards.

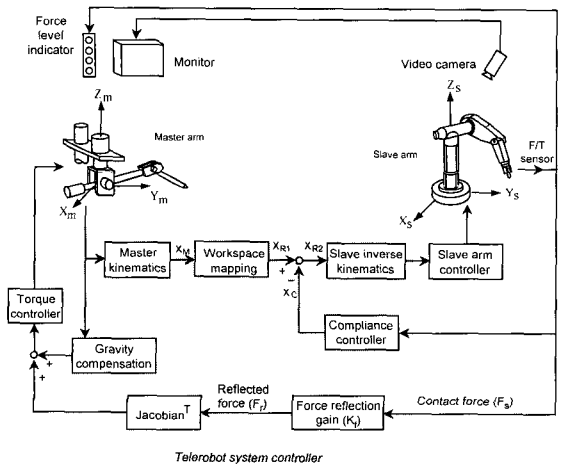

Fig. 1. Structure of the telerobot system.

III. Factors affecting task performance and stability

Fig. 2 shows a typical block diagram of an advanced bilateral controller. The controller consists of a compliance controller and a force reflection gain. The compliance controller constitutes an inner feedback loop, while the force reflection loop forms an outer feedback loop. When contact force occurs, the compliance controller receives this force as input and generates corresponding corrective motion, X_C, as an output. This corrective motion is superimposed on the master arm trajectory, X_{R1}, and as a result, a modified reference trajectory, X_{R2} is generated. At the same time, the contact force is also reflected back to the human operator through the master arm after scaling by a force reflection gain, k_f.

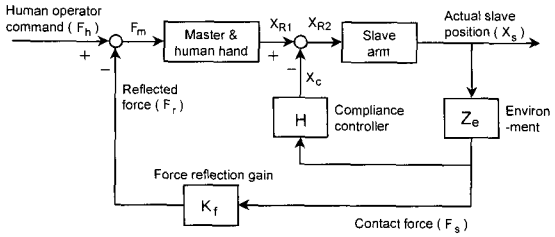

Fig. 2. A typical block diagram of the advanced bilateral control.

1. Effects of the compliance controller

The effect of the compliance controller can be seen to decrease the effective stiffness of a slave arm. The higher the gain of the compliance controller is, the lower the effective stiffness of the slave arm becomes. However, the gain of the compliance controller should be limited because too large gain makes the system unstable. This effect can be shown concisely as in the followings: generally, the slave arm, environments and the compliance controller can be considered as nonlinear systems. If we use the small gain theorem [15] for stability of the compliance loop, which forms a inner feedback loop, the sufficient condition can be obtained by

$$\begin{aligned} &\|[S(X_{R2})]_T\| \le \gamma_1 \|(X_{R2})_T\| \quad \forall T \ge 0,\ \forall X_{R2} \in L_{2e} \\ &\|[H(Z_e(X_S))]_T\| \le \gamma_2 \|(X_S)_T\| \quad \forall T \ge 0,\ \forall X_S \in L_{2e} \\ &\gamma_1 \cdot \gamma_2 \le 1 \end{aligned} \tag{1}$$

where $S(\bullet), H(\bullet)$ and $Z_e(\bullet)$ denote functions for slave, compliance controlller and environments, respectively, while $\|\bullet\|$ denotes the function norm and $(\bullet)_T$ denotes the projection operator.

The above equations mean that the system is BIBO

(Bounded Input Bounded Output) stable if the loop gain is less than unity [16]. To show the effect of the compliance controller more clearly, let the DC gains of S, H and Z_e be denoted by S_0, H_0 and Z_{e0}, respectively, and assume that these gains are remained unchanged during the teleoperation. Then, the DC loop gain, G_{DC} should be less than unity for the system to be stable, i.e.,

$$G_{DC} = H_0 \cdot Z_{e0} \cdot S_0 \le 1 \tag{2}$$

Namely,

$$H_0 \le \frac{1}{Z_{e0} \cdot S_0} \tag{3}$$

From these equations, we can see that a compliance controller must be determined considering the characteristics of the slave arm and the environments, and small compliance would be better to ensure stability. Also, note that the equation (3) does not contain any terms about a force reflection gain or a master arm. It means that we can design a compliance controller without considering or constructing a force reflection loop.

2. Effects of the force reflection gain and the compliance controller

Fig. 3 shows a simplified block diagram of an advanced bilateral control system, where Ψ denotes a compliance loop, i.e., a resultant function of the slave, the environment and the compliance controller. In this system, the contact forces measured by the force/torque sensor are reflected back to the human operator after scaling by a force reflection gain, k_f. This forms a closed loop system and causes a trade-off between task performance and stability.

To concisely investigate the effect of the compliance controller, let us following the similar procedure of the previous section. Let $M(\bullet)$ denote a function for master including human hand, and the DC gains of M and Ψ be denoted by M_0 and Ψ_0, respectively. Then, the DC loop gain, G_{DC} should be less than unity for the system to be stable, i.e.,

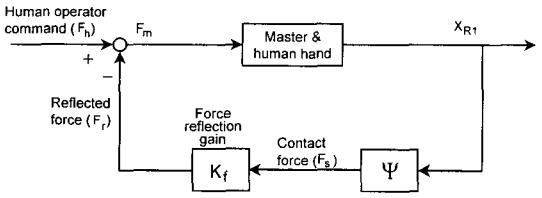

Fig. 3. A simplified block diagram of the advanced bilateral Control.

$$G_{DC} = k_f \cdot \Psi_0 \cdot M_0 \le 1 \tag{4}$$

Considering Ψ_0 denotes the DC gain of a compliance loop, it can be represented as follows:

$$\Psi_0 = \frac{S_0 \cdot Z_{e0}}{1 + S_0 \cdot Z_{e0} \cdot H_0} \tag{5}$$

Substituting this into equation (4) yields

$$G_{DC} = \frac{k_f \cdot S_0 \cdot Z_{e0} \cdot M_0}{1 + S_0 \cdot Z_{e0} \cdot H_0} \le 1 \tag{6}$$

The above equation can be represented as

$$k_f \le \frac{1 + S_0 \cdot Z_{e0} \cdot H_0}{S_0 \cdot Z_{e0} \cdot M_0} \tag{7}$$

These equations show that to ensure stability the force reflection gain must be limited into certain boundary and determined under the consideration of characteristics of the compliance controller, master, the slave, and the environment. Large gain, k_f, can realize big reflected force, but k_f should be limited to satisfy the stable condition of equation (7) Therefore, we can see that there is a trade-off between stability and task performance.

From the above results we can get a useful design guideline of an advanced bilateral controller as follows:

Step 1 : design a compliance controller which satisfies the stable condition of equation (3). Note that the equation does not contain any terms about a force reflection gain or a master arm. It is only related with a slave arm and an environment. This means that we can design a compliance controller without considering or constructing a force reflection loop.

Step 2 : design a force reflection gain which satisfies the stable condition in equation (7). If we design a compliance controller as large as possible in the step 1, the upper bound of k_f can be maximized, which allows the use of the largest k_f.

IV. The Neurofuzzy compliance controller(NFCC)-based control algorithm

1. Structure of the NFCM-based control

Fig. 4 shows overall structure of the proposed scheme. In this scheme the NFCM, which generates corrective motion instead of a conventional compliance controller, automatically determines the suitable compliance for a given task or environment. As shown in the figure, the NFCM consists of two parts. The first one is a fuzzy logic controller(FLC) which receives contact force information as inputs and generates corrective motions as outputs. The second one is a rule learning mechanism which is composed of two neuron-like elements: an associative critic neuron(ACN) and an associative learning neuron(ALN). The mechanism realizes the reinforcement learning algorithm, and thus, trains rule base of the FLC iteratively until the given task can be successfully performed so that no further changes in rules are necessary. When the training has been completed the NFCM can realize suitable compliance for a given task. The failure detector receives contact forces and generates an external reinforcement signal which is used in the rule learning mechanism. The contact force is also reflected back to the human operator through the master arm after scaling by a force reflection gain, k_f. The scheme does not require any prior knowledge on the slave arm dynamics, slave arm controller and the environment. Thus, it can be easily used to the compliance control of a slave arm.

2. Construction of the compliance controller

1) Design of the fuzzy logic controller

The FLC consists four modules: a fuzzy decoder, a rule base, a fuzzy reasoning and a defuzzifier. Before constructing the FLC, let us define the coordinates for force and corrective

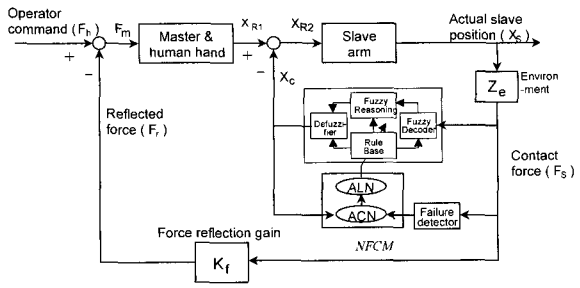

Fig. 4. The block diagram of the proposed algorithm.

motion with respect to the end effector coordinates, $\{O_e\}$, where its origin point, O_e, is in the location of tool center point as shown in Fig. 5. This enables us to derive the FLC without regarding the geometry of working environment. The input and output variables are contact forces, absolute values of change of contact forces and corrective motions. They are defined by

$$\begin{aligned} \boldsymbol{f}(t) &= [f_x(t), f_y(t), f_z(t), m_x(t), m_y(t), m_z(t)]^T \\ &= [f_1(t), f_2(t), f_3(t), f_4(t), f_5(t), f_6(t)]^T \end{aligned} \tag{8}$$

$$\begin{aligned} \Delta f_i(t) &= |f_i(t) - f_i(t-1)| \\ \boldsymbol{c}(t) &= [c_x(t), c_y(t), c_z(t), \theta_x(t), \theta_y(t), \theta_z(t)]^T \\ &= [c_1(t), c_2(t), c_3(t), c_4(t), c_5(t), c_6(t)]^T \end{aligned}$$

where f_i, m_i, c_i and θ_i (i=x,y,z) denote the force, moment, translation and rotation in i-direction with respect to the end effector coordinates, $\{O_e\}$, respectively, while t denotes t-th sampling time.

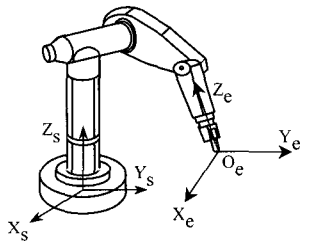

Fig. 5. Definition of an end effector coordinate { O_e }.

a) Fuzzy decoder : The fuzzy decoder inspects the incoming system state and activates the corresponding rules in parallel. These functions are accomplished through fuzzification. From now on, fuzzy variables are discriminated from their crisp variables by adding the tilde sign(~) above the variables. Then, the input fuzzy variables are obtained by scaling from crisp inputs and they are as follows

$$\begin{aligned} \tilde{f}_i &= g_{fi} \times f_i(t) \\ \Delta\tilde{f}_i &= g_{\Delta fi} \times \Delta f_i(t) \qquad (i = 1,2,..,6) \\ \tilde{c}_i &= g_{oi} \times c_i(t-1) \end{aligned} \tag{9}$$

where $g_{fi}, g_{\Delta fi}, g_{oi}$ denote scaling factors for $\tilde{f}_i, \Delta\tilde{f}_i, \tilde{o}_i$, respectively.

b) Rule base : In this study, the output variables of the fuzzy rule takes the form of crisp value, which decreases the calculation time considerably, and thus, profitable in real time application. The rule base takes the form:

$$\begin{aligned} \text{Rule } R_i^k : \text{IF } & \tilde{f}_1 \text{ is } F_1^k,\ \tilde{f}_2 \text{ is } F_2^k,\ \tilde{f}_3 \text{ is } F_3^k,\ \tilde{f}_4 \text{ is } F_4^k,\ \tilde{f}_5 \text{ is } F_5^k,\ \tilde{f}_6 \text{ is } F_6^k, \\ & \Delta\tilde{f}_i \text{ is } \Delta F_i^k, \tilde{o}_i \text{ is } O_i^k \qquad \text{THEN} \qquad \tilde{c}_i \text{ is } C_i^k \\ & (i = 1, 2, .., 6) \qquad (k = 1, 2, .., N) \end{aligned} \tag{10}$$

where the subscript i and the superscript k denote the i-th direction and the k-th rule, respectively. Also, $F_i^k, \Delta F^k, O_i^k$ and C_i^k are fuzzy subsets corresponding to the variables $\tilde{f}_i, \Delta\tilde{f}_i, \tilde{o}_i$ and $\tilde{c}_i$, respectively. Note that C_i^k is not a fuzzy value but a crisp one. In the first, the value of C_i^k is chosen arbitrarily and is learned using the rule learning mechanism described later.

c) Fuzzy reasoning : Fuzzy reasoning is performed using the Min-Max operation. Let $\mu_{C_i^k}(\tilde{c}_i')$ be the membership function for a subset of the output which is the result of the k-th rule. Then it can be obtained by

$$\mu_{C_i^k}(\tilde{c}_i') = [\mu_{F_1^k}(\tilde{f}_1) \wedge \mu_{F_2^k}(\tilde{f}_2) \wedge \cdots \wedge \mu_{F_6^k}(\tilde{f}_6) \wedge \mu_{\Delta F_i^k}(\Delta\tilde{f}_i) \wedge \mu_{O_i^k}(\tilde{o}_i) \wedge \mu_{C_i^k}(\tilde{c}_i)] \tag{11}$$

where $\wedge$ denotes Min operation. From the results of the N rules, the final membership function $\mu_{\tilde{C}_i}(\tilde{c}_i')$ can be obtained by

$$\mu_{\tilde{C}_i}(\tilde{c}_i') = [\mu_{\tilde{C}_i^1}(\tilde{c}_i') \vee \mu_{\tilde{C}_i^2}(\tilde{c}_i') \vee \cdots \vee \mu_{\tilde{C}_i^N}(\tilde{c}_i')] \tag{12}$$

where $\vee$ denotes Max operation.

d) Defuzzifier : In the proposed control scheme, a crisp corrective motion is required. The defuzzifier yields crisp corrective motion from the inferred fuzzy corrective motion. The crisp corrective motion, c_i, can be obtained by

$$c_i = g_{ci} \times \text{Deffuzify}\{\mu_{\tilde{C}_i}(\tilde{c}_i')\} \tag{13}$$

where g_{ci} are scaling factors for $\tilde{c}_i$ and Deffuzify{•} denotes the defuzzifier operator.

2) Rule learning mechanism

The objective of rule learning is to learn the output linguistic values of C_i^k in the rule base. Such a learning capability is performed by the rule learning mechanism, which consists of two neuron-like elements: the associative critic neuron and the associative learning neuron. The rule learning mechanism is based upon the reinforcement learning algorithm [12]-[13], and the detailed algorithm is similar to that described in [5].

3) Failure detector

The failure detector receives contact forces as inputs and generates an external reinforcement signal as an output. When a given task is performed successively, the external

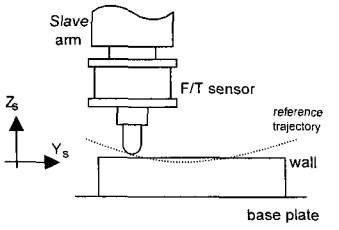

Fig. 6. A wall contacting task

reinforcement signal has a value more than zero, and in the opposite case, its value is less then zero. Other sensory information except contact force also may be used to generate the reinforcement signal. The objective of this detector is to determine whether the task is performed successively or not. Therefore, construction of a failure detector is rather heuristic and completely depends on a given task.

3. Construction of the force reflection controller

The reflected force is evaluated by multiplying the contact force by the force reflection gain, as shown in Fig. 1. The resultant is then converted to the torque applied at each axis of master arm through the transpose of the master Jacobian. The force reflection gain should satisfy the stable condition in equation (7).

V. Experiments and Results

To investigate effectiveness of the proposed scheme, a series of experiments has been carried out using the telerobot system shown in Fig. 1. A wall contacting task shown in Fig. 6 was performed as an example task. A steel peg was attached at the end of the slave arm, and a plastic wall was located in the lower side. The reference trajectory was assigned through the master arm as shown in the figure. During the experiments the direction of the end effector is fixed to a constant (-Z_S direction) with respect to the global reference coordinates. Among the contact forces, the three dimensional moments are small compared to the three dimensional force. In this study, therefore, for simplicity the proposed control scheme is implemented for the three directional forces only.

1. Construction of an NFCM

Inputs for the NFCM are the three directional forces, f_i, the change in the forces, Δf_i, and one-step-ahead corrective motions, O_i, while the outputs are the corrective motions, c_i, $(i = x, y, z)$. The rule base is as follows :

$$\begin{aligned}
\text{Rule } \mathrm{R}_1^k &: \text{IF } \tilde{f}_1 \text{ is } \mathrm{F}^k,\ \tilde{f}_2 \text{ is } \mathrm{G}^k,\ \tilde{f}_3 \text{ is } \mathrm{G}^k, \\
&\quad \Delta\tilde{f}_1 \text{ is } \Delta\mathrm{F}^k,\ \tilde{o}_1 \text{ is } \mathrm{O}^k \text{ THEN } \tilde{c}_1 \text{ is } \mathrm{C}_1^k \\
\mathrm{R}_2^k &: \text{IF } \tilde{f}_1 \text{ is } \mathrm{G}^k,\ \tilde{f}_2 \text{ is } \mathrm{F}^k,\ \tilde{f}_3 \text{ is } \mathrm{G}^k, \\
&\quad \Delta\tilde{f}_2 \text{ is } \Delta\mathrm{F}^k, \tilde{o}_2 \text{ is } \mathrm{O}^k \text{ THEN } \tilde{c}_2 \text{ is } \mathrm{C}_2^k \\
\mathrm{R}_3^k &: \text{IF } \tilde{f}_1 \text{ is } \mathrm{G}^k,\ \tilde{f}_2 \text{ is } \mathrm{F}^k,\ \tilde{f}_3 \text{ is } \mathrm{G}^k, \\
&\quad \Delta\tilde{f}_3 \text{ is } \Delta\mathrm{F}^k, \tilde{o}_3 \text{ is } \mathrm{O}^k \text{ THEN } \tilde{c}_3 \text{ is } \mathrm{C}_3^k \\
&\qquad\qquad (\mathrm{k} = 1, .., 120)
\end{aligned} \tag{14}$$

where k denotes the k-th rule. The input linguistic values are defined as shown in Fig. 7. Table 1 shows the scaling factors for $g_{fi}, g_{\Delta fi}, g_{oi}$ and g_{ci}. Each set of rules, $\mathrm{R}_1^k, \mathrm{R}_2^k$ and R_3^k, is composed of 120 ($5\times2\times2\times2\times3$) rules.

Table 1. The scaling factors for the input and output variables.

g_{f1}	0.05	g_{o1}	0.167
g_{f2}	0.05	g_{o2}	0.167
g_{f3}	0.025	g_{o3}	0.333
$g_{\Delta f1}$	0.5	g_{c1}	1.0
$g_{\Delta f2}$	0.5	g_{c2}	1.0
$g_{\Delta f3}$	1.0	g_{c3}	2.0

The goal of the experiment is to make the slave arm as compliant as possible so as to maximize the force reflection gain. Thus, a failure detector is designed to have three rules as follows

$$\begin{aligned}
&\text{Rule 1} : \text{IF} \quad f(t) > f_{\max} \quad \text{THEN } \textit{fail} \\
&\text{Rule 2} : \text{ELSE IF} \quad |f(t) - f(t\text{-}1)| > delf_{\max} \quad \text{THEN } \textit{fail} \\
&\text{Rule 3} : \text{ELSE} \quad \textit{success}
\end{aligned} \tag{15}$$

where $f(t)$ is defined as follows

$$f(t) = \sqrt{f_1^2 + f_2^2 + f_3^2} \tag{16}$$

where $f_{\max}$ = 50N and $delf_{\max}$ = 3N, while the value for *success* = 0.055 and *fail* = -0.055. Rule 1 checks whether the learning process is proceeding to minimize the contact force, and Rule 2 checks whether the contact state is stable or not.

2. Learning of the NFCM

Since we can design a compliance controller without considering or constructing force reflection, the contact force was not reflected to the human operator during the learning process. In other words, only the compliance controller was used. Experiments were conducted in the following manner: a human operator performed the wall contacting task many times. During the operation three trajectories shown in Fig. 8 were stored in the computer, and these were subsequently assigned to the slave arm as references in the order of (1)-(2)-(3)-(1)-(2)-(3)....

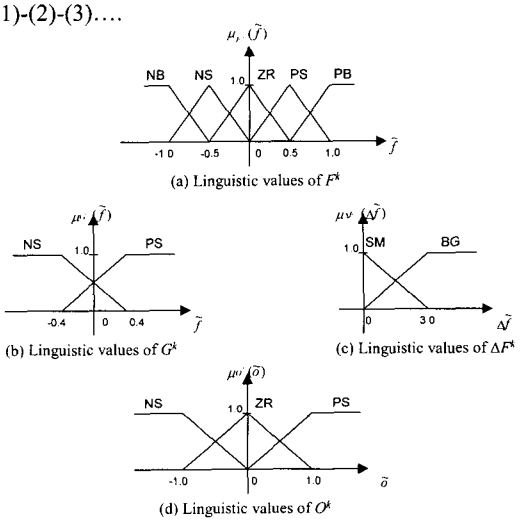

(a) Linguistic values of F^k

(b) Linguistic values of G^k

(c) Linguistic values of ΔF^k

(d) Linguistic values of O^k

Fig. 7. Definition of the fuzzy linguistic values.

A learning operation consists of a training task and an evaluation task. At the first operation, a task following the trajectory (1) is performed as a *training task*. During this task the contact force occurs as the peg contacts the wall. The fuzzy logic controller, then, generated corrective motion. At the same time the rule learning mechanism is activated, and thus the output linguistic values, C_i^k, are trained. After this, a

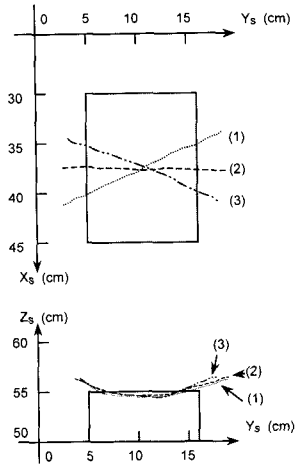

Fig. 8. Various reference trajectories.

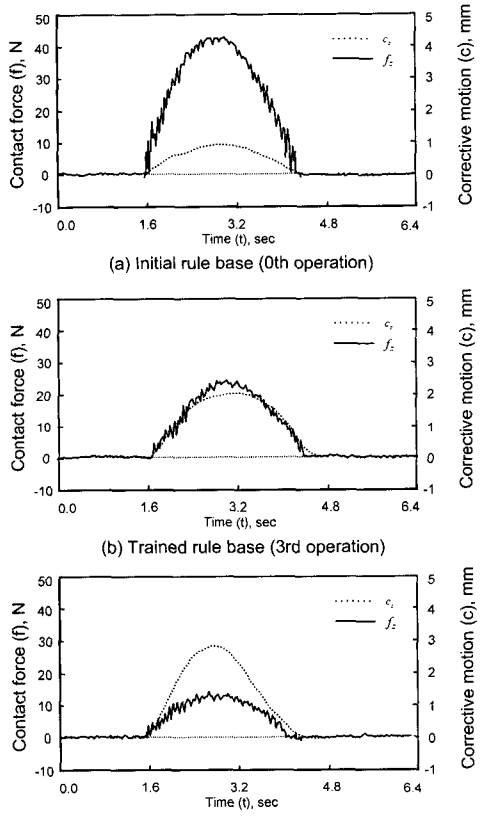

Fig. 9. Z-directional contact forces and corresponding corrective motions.

task of following trajectory (3) is performed as an *evaluation task*, to evaluate the effect of rule learning. During the evaluation task, the rule learning mechanism is not activated, and thus the rules are not changed. At the second and third operations, trajectories (2) and (3) are assigned as references during the training tasks, respectively. At every operation, the evaluation task with trajectory (3) is followed by the training task. At the forth operation, trajectory (1) is used again as a reference and for the next, trajectories (2), (3), .. are successively assigned. These operations were repeated until no further changes occur in the rule base.

Table 2. Changes of the rule base for x-axis.
(in the case of $\Delta\tilde{f}_1 = \mathrm{SM}$, $\tilde{f}_2 = \mathrm{NS}$ and $\tilde{f}_3 = \mathrm{NS}$)

C_1^k		O^k NS	ZR	PS
F^k	NL	-1.2	-0.2	0.4
	NS	-1.0	-0.1	0.6
	ZR	-0.8	0.0	0.8
	PS	-0.6	0.1	1.0
	PL	-0.4	0.2	1.2

(a) Initial rule base

C_1^k		O^k NS	ZR	PS
F^k	NL	-1.62	-0.37	0.46
	NS	-1.44	-0.24	0.70
	ZR	-1.30	0.00	1.21
	PS	-0.74	0.19	1.48
	PL	-0.65	0.33	1.53

(b) 3rd operation: plastic wall

C_1^k		O^k NS	ZR	PS
F^k	NL	-2.17	-0.51	0.52
	NS	-1.76	-0.23	0.84
	ZR	-1.39	0.00	1.44
	PS	-1.11	0.27	1.65
	PL	-0.84	0.46	1.79

(c) 9th operation: plastic wall

C_1^k		O^k NS	ZR	PS
F^k	NL	-1.69	-0.18	0.50
	NS	-1.42	-0.10	0.61
	ZR	-1.31	0.00	0.78
	PS	-0.83	0.22	1.05
	PL	-0.70	0.31	1.39

(d) 9th operation: steel wall

The z-directional results of the evaluating tasks for the third and ninth operations are shown in Fig. 9. In the figure, the 0 (zero) th evaluation task represents the results with the initial rule base. Fig. 10 shows the maximum forces generated during each evaluation task, and Table 2(a)-(c) shows change of the rule bases for x-axis in the case of $\Delta\tilde{f}_1 = \mathrm{SM}$, $\tilde{f}_2 = \mathrm{NS}$ and $\tilde{f}_3 = \mathrm{NS}$. From the table we can see that the rule base is changed as the learning goes on. Changes of the rule bases for the y and z-axes and other cases on the x-axis are similar, and thus are not presented here. A careful analysis of these results reveals that, in the early stages, the linguistic values increase with the number of operations. Therefore, the corrective motion also increases. This yields a decrease in the maximum force. However, all of these become stationary as the number of operations becomes large. Thus, it can be seen that the NFCM can generate suitable compliance with the aid of the rule-learning mechanism.

Another set of experiment was performed using a steel wall which is much stiffer than the plastic one, while its dimensions and location are kept the same as the above experiments. The other conditions were also set identically to the above experiments. The results are shown in Fig. 10 and Table 2(d). From the results we can see that the learning process shows a similar tendency to that of the previous one: as the operations goes on,

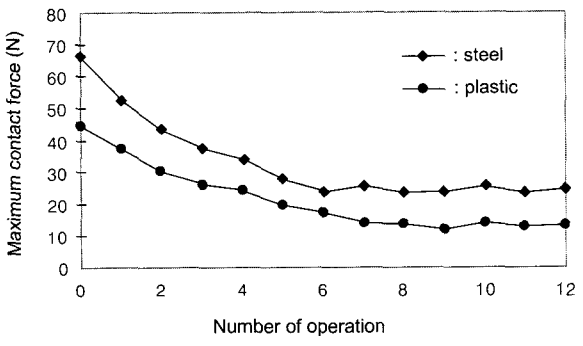

Fig. 10. Change of maximum contact forces in z-direction.

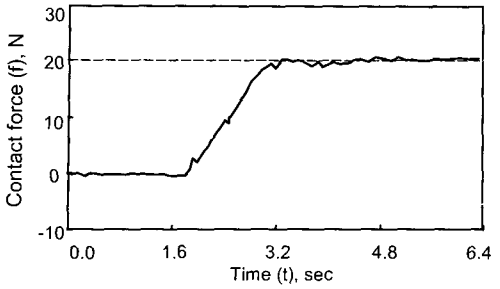

(a) NFCM-based bilateral control

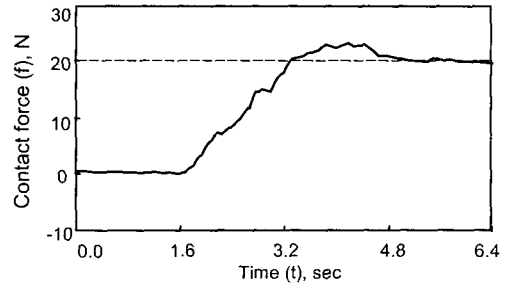

(b) Kim's advanced bilateral control

Fig. 11. Results of the wall contacting experiments.

the linguistic values and the corrective motion increase, and contact force decreases. All of these also become stationary as the number of operation becomes large. In case of steel, however, the contact force gets larger during all operations and the final linguistic values are smaller than those of the plastic one. This means that the NFCM can realize smaller compliance than that in case of plastic. Since all the experimental conditions except the material of the wall are the same as those of the previous experiment, it can be concluded that such differences arise from the difference in the environment.

The fact, which the NFCM can realize larger compliance in plastic wall than that in steel wall, complies with Waibel's result [17], where it is reported that in order to guarantee stability for a given robot position controller, the gains of a compliance controller must be decreased as the stiffness of the environment increases. In other words, for a more compliant environment, a compliance controller can produce more compliance, and thus, can achieve a smaller contact force. Thus it can be seen that the NFCM is capable of providing suitable compliance, corresponding to the various types of environment.

3. NFCM-based advanced bilateral teleoperation

An NFCM-based bilateral controller was constructed using the learned NFCM and the force reflection controller described in section 4.3. The force reflection gain was experimentally set to 0.3, which was the maximum allowable gain in the stable region. The task was to maintain a constant contact force of 20N in z-direction to the plastic wall shown in Fig. 8, and the results are shown in Fig. 11(a). From the figure it can be seen that the contact occurred at about 1.7 sec. Note that after the contact, the compliance controller generated corrective motion according to the contact force, and at the same time the force was also fed back to the human operator. After 3.2 sec contact forces were very close to the desired value, 20N. Since it was controlled by a human operator, the results did not show exact 20N.

To compare the results with those of another algorithm, the same task was conducted using Kim's algorithm [8]. The gains of the compliance controller was tuned so as to make the slave arm as compliant as possible. The force reflection gain was experimentally set to 0.2, which was also the maximum allowable gain in the stable region. From the results shown in Fig. 11(b) it can be seen that the contact force is a little oscillatory, and becomes about 20N after 5 sec. From the above results, it can be seen that the proposed algorithm shows better task performance.

VI. Conclusions

The paper presented a novel method for design of an advanced bilateral controller. The factors affecting task performance and stability in the advanced bilateral controller were analyzed and a design guideline was presented. The neuro-fuzzy compliance model (NFCM)-based bilateral control proposed herein is an algorithm designed to automatically determine the suitable compliance for a given task or environment. The NFCM, composed of a fuzzy logic controller (FLC) and a rule-learning mechanism, is used as a compliance controller. The FLC generates compliant motions according to contact forces. The rule-learning mechanism, which is based upon the reinforcement learning algorithm, trains the rule-base of the FLC until the given task is done successfully. Since the scheme allows the use of large force reflection gain, it can ensure good task performance. Moreover, the scheme does not require any priori knowledge on a slave arm dynamics, a slave arm controller and an environment, and thus, it can be easily applied to the control of any telerobot systems. The effectiveness of the proposed algorithm was verified through a series of experiment.

In this study automatic selection of force reflection gain is not dealt with. Development of an algorithm that can automatically determine both a compliance controller and a force reflection gain would assure better task performance and is now under investigating.

References

[1] D. H. Cha and H. S. Cho, " Neural network and fuzzy logic systems: Techniques and applications in telerobot systems," in *Fuzzy Theory Systems Techniques and Applications*, Ed. C. T. Leondes, Academic Press, pp. 1129-1179, 1999

[2] A. K. Bejczy and W. S. Kim, "Predictive displays and shared compliance control for time delayed telemanipulation," *Proc. IEEE/RSJ Int. Workshop on Intelligent Robots and Systems*, pp. 407-412, 1990.

[3] W. S. Kim, "Shared compliant control: A stability analysis and experiments," *Proc. IEEE Int. Conf. Robotics and Automation*, pp. 620-623, 1990.

[4] K. Kosuge, A. Sato and K. Furuta, "Task-oriented control of master-slave manipulators," *Proc. Japan-U.S.A. Sym.*

on Flexible Automation, pp. 387-393, 1990.

[5] D. H. Cha and H. S. Cho, "A neurofuzzy model-based compliance controller with application to a telerobot system," *Control Engineering Practice*, vol. 4, no. 3, pp. 319-330, 1996.

[6] B. Hannaford and R. Anderson, "Experimental and simulation studies of hard contact in force reflecting teleoperation," *IEEE Int. Conf. Robotics and Automation*, pp. 584-589, 1988.

[7] G. J. Raju, G. C. Verghese and T. B. Sheridan, "Design issues in 2-port network models of bilateral remote manipulation," *Proc. IEEE Int. Conf. Robotics and Automation*, pp. 1316-1321, 1989.

[8] W. S. Kim, "Developments of new force reflecting control schemes and an application to a teleoperator training simulator," *Proc. IEEE Int. Conf. Robotics and Automation*, pp. 1412-1419, 1992.

[9] B. Hannaford, "Stability and performance tradeoffs in bilateral telemanipulation," *IEEE Int. Conf. Robotics and Automation*, pp. 1764-1767, 1989.

[10] A. A. Goldenberg, and D. Bastas, "On the bilateral control of force reflecting teleoperation," *Proc. 11th IFAC World Congress*, pp. 215-220, 1990.

[11] D. H. Cha and H. S. Cho, "Design of a neurofuzzy algorithm-based shared controller for telerobot systems," *Robotica*, Vol. 15, No. 1, pp. 11-22, 1997.

[12] A. G. Barto, R. S. Sutton and C. W. Anderson, "Neuronlike adaptive elements that can solve difficult learning control problems," *IEEE Trans. Systems, Man and Cybernetics*, vol. 13, no. 5, pp. 834-846, 1983.

[13] C. C. Lee, "A self-learning rule-based controller with approximate reasoning and neural nets," *Proc. IFAC '90 World Congress*, vol. 7, pp. 59-64, 1990.

[14] D. H. Cha, *Shared control of telerobot systems using artificial intelligence algorithms*, Ph. D. Dissertation, Korea Advanced Institute of Science & Technology, 1995.

[15] C. A. Desore and M. Vidyasagar, *Feed-back systems: Input-output properties*, New York: Academic Press, 1975.

[16] F. L. Lewis, C. T. Abdallah and D. M. Dawson, *Control of robot manipulators*, Macmillan Publishing, 1993.

[17] B. J. Waibel and H. Kazerooni, "Theory and experiments on the stability of robot compliance control," *IEEE Trans. Robtotics and Automation*, vol. 7, no. 1, pp. 95-104, 1991.

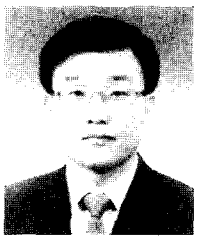

Dong-hyuk Cha

He received the B.S. degree in Mechanical design from Seoul National University in 1984, and the M. S. and Ph. D. degrees in Mechanical Engineering from KAIST in 1986 and 1995, respectively. From 2000 to 2001 he was a visiting professor at University of Pennsylvania. Since 1998 he has been an Assistant Professor of Control and Measurement Engineering in Korea Polytechnic University. His fields of research are intelligent robotics, control and automation of manufacturing processes.

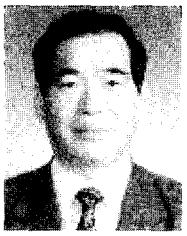

Hyung Suck Cho

He received the B.S. degree in industrial education (Mechanical Engineering) from Seoul National University, Seoul, Korea, the M.S. degree in mechanical engineering from Northwestern University, Evanston, IL, and the Ph.D. degree in mechanical engineering from the University of California at Berkeley, CA, in 1971, 1975, and 1977 respectively. His fields of research are intelligent control and robotics, machine vision and its application, and manufacturing process monitoring and control. Dr. Cho is a Fellow of Korea Academy of Science and Technology, Korea and also a member of ASME, IEEE, SPIE, SME, KAST, KSPE, and KSME.